Lycopodium root meristem dynamics supports homology between shoots and roots in lycophytes

Lycopodium root meristem dynamics supports homology between shoots and roots in lycophytes

Rieko Fujinami, Atsuko Nakajima, Ryoko Imaichi,

Toshihiro Yamada

Fujinami, R., Nakajima, A., Imaichi, R., & Yamada, T. (2020). Lycopodium root meristem dynamics supports homology between shoots and roots in lycophytes. *New Phytologist*, 229(1), 460–468. https://doi.org/10.1111/nph.16814

Lycopodium root meristem dynamics support homology between shoots and roots in lycophytes

Rieko Fujinami[1] (https://orcid.org/0000-0001-5344-181X), Atsuko Nakajima[2], Ryoko Imaichi[2], Toshihiro Yamada[3] (https://orcid.org/0000-0002-9064-7048)

[1]Faculty of Education, Kyoto University of Education, 1 Fujinomori-cho, Fukakusa, 612-8522, Kyoto, Japan. [2]Department of Chemical and Biological Sciences, Japan Women's University, Mejirodai, Tokyo 112-8681, Japan. [3]Botanical Gardens, Faculty of Science, Osaka City University, Kisaichi, Katano, Osaka 576-0004, Japan.

Author for correspondence

Toshihiro Yamada

E-mail: ptilo@nifty.com, phone: +81-72-891-2751

Total word count (excluding summary, references and legends):	3797	No. of Figures:	3 (all in color)
Summary:	188	No. of Tables:	2
Introduction:	667	No. of Supporting Information files:	9(Fig. S1–S5; TableS1–S4)
Material and methods:	1293		
Results:	1125		
Discussion:	683		
Acknowledgements:	29		

Summary

- Roots played a pivotal role in the conquest of land by vascular plants, yet their origin has remained enigmatic. Palaeobotanical evidence suggests that roots may have originated from subterranean shoots in some lycophyte species. If this hypothesis is correct, it would follow that the roots and shoots of extant lycophytes share fundamental developmental mechanisms.
- We tracked meristem dynamics in root and shoot apices of *Lycopodium clavatum* using a thymidine analogue and expression patterns of *histone H4*, respectively. Then we compared the meristem dynamics of roots and shoots to identify developmental similarities.
- Both apical meristems contained a quiescent tissue characterised by a low frequency of cell division. Actively dividing cells appeared in the quiescent tissue during dichotomous branching of both roots and shoots. As a result, the parental meristem divides into two daughter meristems, which give rise to new root or shoot apices.
- These striking similarities in meristem dynamics provide new neobotanical data that support the shoot-origin hypothesis of lycophyte roots. Although *Lycopodium* roots may have originated from subterranean shoots of Devonian lycophytes, these shoots may have changed into root-bearing axes in other extant lycophyte lineages.

Key words: dichotomous branching, lycophytes, Lycopodiaceae, *Lycopodium*, meristem, quiescence, root origin

Introduction

Extant vascular plants have belowground roots that facilitate the uptake of water and water-soluble nutrients and anchor plants to their substrates (Esau, 1965; Gifford & Foster, 1989). Despite their present-day functional similarities, roots likely evolved at least twice in vascular plants; fossil records indicate that lycophytes and euphyllophytes (ferns and seed plants) diverged before the origin of roots (Raven & Edwards, 2001; Friedman *et al.*, 2004; Kenrick & Strullu-Derrien, 2014; Hetherington & Dolan, 2017, 2019). In the Early Devonian landscape, roots would have provided a significant advantage to plants, allowing them to access inorganic salts and penetrable substrates that had become increasingly available through rapid weathering of the earth's rocky surface (Raven & Edwards, 2001; Le Hir *et al.*, 2011). Thus, the parallel evolution of roots between lycophytes and euphyllophytes highlights the importance of roots to early vascular plants, yet, the origin of roots remains controversial.

Lycophytes, consisting of lycopsids and polyphyletic zosterophylls (Kenrick & Crane, 1997), may have been the first group to acquire roots (Hao *et al.*, 2010; Matsunaga & Tomescu, 2016, 2017). Roots likely evolved in lycophytes several times (Rothwell & Erwin, 1985; Fujinami *et al.*, 2017, 2020), in some cases from subterranean stems (rooting axes) of species in the earliest lycopsid order,

Drepanophycales, through the acquisition of a root cap (Kidston & Lang, 1921; Gensel & Berry, 2001; Gensel *et al.*, 2001; Hetherington & Dolan, 2018, 2019). This hypothesis suggests that roots may be homologous to stems in extant lycophytes related to Drepanophycales, although exact relationships between extant lycophyte families (Lycopodiaceae, Selaginellaceae, and Isoetaceae) and Drepanophycales are not fully understood (Kenrick & Crane, 1997; Doyle, 1998). However, a close link in body plans, as well as a possible phylogenetic tie (Kenrick & Crane, 1997), is often suggested between Drepanophycales and extant Lycopodiaceae because they share morphological characters such as the alternate arrangement of fertile and sterile zones on the shoot axis, amorphous sporopollenin layer localized around the spore aperture, and degeneration of cytoplasm in tapetum cells before spore maturation (Kerp *et al.*, 2013). Notably, the shoot apical meristems (SAMs) of the drepanophycalean *Asteroxylon mackiei* had a mass of initial cells (Hueber, 1992), much like the SAMs of Lycopodiaceae (Clowes, 1961; Imaichi, 2008). In addition, the apical meristems of *Asteroxylon* rooting axes had a similar tissue organisation to the root apical meristems (RAMs) of some extant Lycopodiaceae in that there was a mass of initial cells in the meristem (Hetherington & Dolan, 2018, 2019; Fujinami *et al.*, 2020). Thus, among the

three extant lycophyte families, Lycopodiaceae is an excellent taxon upon which to test the shoot-origin hypothesis for roots.

If Lycopodiaceae roots follow the above-described paleobotanical scenario, then fundamental developmental mechanisms should be shared between RAMs and SAMs, as these tissues are the ultimate source of roots and shoots, respectively. Lycopodiaceae have shoot and root systems branched in an equally dichotomous (isotomous) or unequally dichotomous (anisotomous) manner (Imaichi, 2008; Kenrick & Strullu-Derrien, 2014), as did their Devonian ancestors (Kenrick & Crane, 1997; Gensel & Berry, 2001; Matsunaga & Tomescu, 2016, 2017; Poschmann *et al.*, 2020). Many anatomical studies have been conducted on the shoots and roots of Lycopodiaceae to illustrate tissue organisation in apical meristems (e.g., Clowes, 1961; Imaichi & Kato, 1989; Barlow, 1995; Otreba & Gola, 2011); these analyses are essential for comparing RAMs and SAMs. However, the classical techniques employed in these studies could not demonstrate cell division frequencies, which are necessary to clarify tissue organisation. Therefore, it remains unclear if shoots and roots employ similar mechanism(s) for dichotomous branching because meristematic dynamics have not been traced during the branching process.

To clarify meristematic dynamics during shoot and root branching, we monitored cell division activities in the club moss *Lycopodium clavatum* (Lycopodiaceae) using molecular markers for DNA replications. We compared RAMs and SAMs to determine if they shared the following attributes: 1) the presence of quiescent tissue, which is characterised by a low cell division frequency, and 2) a parental apical meristem splitting to form two daughter meristems during dichotomous branching.

Materials and Methods

Collection of *Lycopodium clavatum* and root architecture observations

Shoots and roots of *Lycopodium clavatum* L. (Fig. S1a) were collected in Takao, Kyoto, Japan. Voucher specimens were stored in the herbarium at the National Museum of Nature and Science, Tokyo. *Lycopodium* root systems usually contain two thick second-order roots from which third-order roots are anisotomously branched (Fig. S1b–e). For root architecture observations, we collected young root systems that included up to eight third-order roots (Fig. S1b–d) and measured the distance between the first two third-order roots (Fig. S1b). We examined the branching patterns of 72 first-order and 124 second-order roots in total (Table S1).

EdU labelling and DAPI staining of RAMs

To track meristem dynamics during root branching, we mainly observed first-order roots because they are usually intact. In *L. clavatum*, branching patterns varied considerably among roots after their endogenous origination; some already had two incipient daughter RAMs when they broke from the parent stem, whereas others had not branched yet. This variability made it difficult to define branching stages according to root age. Therefore, we used root tip width/length ratios for staging since the tips generally become broader to accommodate two new apices during branching (Imaichi & Kato, 1989; Yi & Kato, 2001). Roots were classified into two categories based on this ratio, i.e., < 4 (stage 0) and ≥ 4 (stage I) when only one quiescent centre-like tissue (QCL) was recognisable from the outside (Fujinami *et al.*, 2017; Fig. S1f–k). Roots were assigned to stage II if two incipient daughter QCLs were recognisable in a root tip. Because QCLs are less transparent than the surrounding tissues, we were able to count them externally by transmitting light through the root tips. Root width was measured at the level of differentiating procambial cells (upper dotted line, Fig. S2); length was defined as the distance from this level to the bottom of the QCL.

We incorporated 5-ethynyl-2′-deoxyuridine (EdU) into DNA during the S phase of cell division as a thymidine analogue. Root tips were observed for each stage of root

branching (Fig. S2; Tables 1, S2). We incorporated and detected EdU, and performed counterstaining with 4',6-diamidino-2-phenylindole (DAPI) to count nuclei, as previously described (Fujinami *et al.*, 2017). Root tips with EdU labelling were fixed with 4.0% paraformaldehyde in 0.1 M phosphate buffer (pH 7.2) at 4°C overnight, embedded in Technovit 7100 (Heraeus Kulzer), and cut into sections of 2 μm thickness. A longitudinal median section of each root was used for DAPI staining and EdU detection, and these images were superimposed for counting nuclei. Four sections adjacent to the median one (two front and two behind) were also used for EdU detection to confirm presence of the QCL. As in our previous study (Fujinami *et al.*, 2017), QCL nuclei were counted in a region inside the initial cell layers (Fig. S1f–k), whereas those of the root tip were counted between the level of procambium differentiation and the outermost layer of the intact root cap (dotted lines, Fig. S2). The lower line is set to exclude cells that were starting to fall from the root cap. To calculate the cell division frequency, we divided the number of EdU-positive nuclei by that of DAPI-stained nuclei.

For anatomical observations, sections were stained with modified Sharman's staining solution (Jernstedt *et al.*, 1992) after EdU or DAPI observations.

Gene isolation

Total RNA was extracted from shoots of *L. clavatum* and cDNA was prepared as previously described (Yamada *et al.*, 2011). Partial coding sequences of the Class I *KNOTTED*-Like Homeobox (*KNOX I*) gene and *histone H4* homologues were amplified by polymerase chain reaction (PCR) based on the cDNA (Table S4). The identity of the isolated *histoneH4* homologue was confirmed using the BLAST X search tool, which is available on the National Center for Biotechnology Information (NCBI) website (https://www.ncbi.nlm.nih.gov/).

Two candidates for the *KNOX I* gene were isolated; their phylogenetic positions within the *KNOX I* and Class II *KNOTTED*-Like Homeobox (*KNOX II*) genes were verified. Amino acid sequences translated from these two genes were aligned with those of other KNOX proteins using the MEGA X software (Kumar *et al.*, 2018) and poorly aligned regions were eliminated using the Gblock software (Talavera & Castresana, 2007) allowing 1) smaller final blocks, 2) gap positions within the final blocks, and 3) less strict flanking positions. Phylogenetic analysis was conducted based on the neighbour-joining method using MEGA X; the Jones–Taylor–Thornton model was selected, with a Gamma parameter of 1.00. Support for each node was tested with 1,000 bootstrap replicates. One of the isolated genes was included in a clade of *KNOX I* genes

(*LcKNOX I*, Fig. S3); this gene was therefore used for *in situ* hybridisation analyses.

The nucleotide sequences newly determined in this study were registered in the DNA Data Bank of Japan (DDBJ), European Molecular Biology Laboratory (EMBL), and NCBI databases as *LcHistoneH4* (LC500884), *LcKNOX I* (LC500886), and *LcKNOX II* (LC500887). The alignment data used in this study are available from the corresponding author upon request.

In situ hybridisation

As in roots, relative stages of shoot branching can be defined according to width/length ratios of the shoot tips because shoot tips expand laterally toward dichotomy (Imaichi & Kato, 1989; Yin & Meicenheimer, 2017). Accordingly, we classified shoots without external signs of branching into those with ratios of < 3.0 (stage 0) and ≥ 3.0 (stage I). Stage I shoots were further classified based on cell numbers in SAM (see below for counting procedure); i.e., < 250 (stage IA) and ≥ 250 (stage IB), with the larger class representing the later stage. We classified shoots into stage II if a young daughter shoot apex was clearly visible from the outside (Fig. S4; Tables 2, S3). We measured shoot width just above the first leaf for shoots at stage 0 or stage I, and at the level of the sinus between the main and daughter apices for shoots at stage II. Length was defined as the

distance from the apex to the level of width measurement.

Shoot and root tips were fixed in 50% ethanol/formaldehyde/acetic acid (FAA; 17:2:1 by volume) at 4°C for 12 h and embedded in Paraplast plus (Oxford Labware) via an ethanol and t-butyl alcohol series. Antisense- and sense-strand (control) probes were synthesised from a partial coding sequence (see above) of *LcKNOX I* or *LcHistoneH4* inserted into the pGEM-T vector (Promega) using primers shown in Table S4. Embedded samples were sectioned at a thickness of 8 μm and each of four serial sections was hybridised with *LcKNOX I* antisense-strand, *LcHistoneH4* antisense-strand, or one of their sense-strand probes. Hybridisation with probes and subsequent detection of hybridised probes were performed as previously described (Yamada *et al.*, 2011). Images of the negative controls are shown in Fig. S5a–j. Cells in the *LcKNOX I*-expressing region and *LcHistoneH4* expression blank were counted per SAM and organising centre-like tissue (OCL), respectively (Fig. S4; Table S3). Images of the *LcKNOX I* and *LcHistoneH4* results were superimposed to specify SAM and OCL regions and cells were counted on the closer of the two images to the median longitudinal section. To calculate cell division frequency, we divided the number of *histone H4*-stained cells by the total number of cells in the tissue.

Cell division was visualised by EdU staining in roots (Fujinami *et al.*, 2017) and

histone H4 expression in shoots due to the technical difficulty in administering EdU to shoots. Both EdU labelling (Salic & Mitchison, 2008) and *histone H4* expression patterns (Brandstädter *et al.*, 1994; Kouchi *et al.*, 1995; Meshi *et al.*, 2000) were used to detect cells in the S phase; these methods reproduce comparable patterns in barley RAMs (Kirschner *et al.*, 2017). We confirmed the comparability of these two methods in RAMs of *L. clavatum* (Fig. S5k–m).

Results

Parental RAM splits into two daughter RAMs

Root primordia arose endogenously and 94% of emerging first-order roots branched isotomously to form second-order roots of equal size (Fig. 1a). Subsequently, two anisotomous dichotomies occurred successively, resulting in one large second-order root and two small third-order roots (Fig. 1b, c). The interval between the first pair of third-order roots was < 1 mm in 58% and 1–2 mm in 19% of the second-order roots, respectively (Fig. 1d; Table S1). These short intervals made an appearance like trichotomous branching (Fig. 1b, c). The second- and third-order roots repeatedly underwent anisotomous branching to form complex root systems; pairs of successive anisotomies were frequently observed (Fig. S1c–e).

We then tracked cell division dynamics during the first dichotomous root branching in RAMs using EdU staining to determine how daughter RAMs are formed. RAMs of *L. clavatum* contain tissue with a relative low frequency of cell division (Figs 1e, f, S2a–d; Table 1) (Fujinami *et al.*, 2017), which resembles the quiescent centre (QC) found in seed plants (Dolan *et al.*, 1993; van den Berg *et al.*, 1997). QCL is a mass of cells surrounded by initial cell files that radiate outward to supply cells to the root body and cap (Fig. S1f–k; Fujinami *et al.*, 2017). The QCL was persistent throughout root branching (Fig. 1e–q; Table 1).

From stage 0 to stage I, the number of nuclei increased in the root tips (Table 1), confirming that stage I represented the older branching stage. Width/length ratios in the QCL also increased at this stage transition (compare Fig. 1e, f with 1g, h; Table 1), which is consistent with the broadening of the root tip. In three of seven roots observed in stage I (+EdU column in Table 1), a group of cells with active EdU incorporation appeared in the centre of the QCL (Figs 1i, j, S2i–k). These three roots included more nuclei in the QCL and root tips than the other four roots (-EdU column in Table 1). These increases suggest that +EdU roots are slightly older than -EdU roots within stage I.

Around the position of these EdU-positive cells, seven or eight initial cell files

were developed at stage II (Fig. S1i, j). These cell files separated the two incipient daughter RAMs, each of which contained a group of cells with reduced EdU incorporation (Fig. 1k, l; Table 1). We were not able to track the distances between the two daughter RAMs over time, but two RAMs should be pulled apart as these cell files become broader by anticlinal cell division (Figs 1m, n, S1i–k, S2l–p).

We also observed EdU incorporation in second-order roots during anisotomous branching because this branching pattern is unusual among extant lycophytes (Imaichi, 2008). During the pairs of successive anisotomies, two groups of EdU-labelled cells were observed in the parental QCL (Fig. 1o, p), which would separate the parental QCL into one central large and two small daughters. Therefore, anisotomous and isotomous dichotomies occur in the same manner, except that the sizes of the resulting daughter QCLs are unequal in the former.

These data suggest that fission of the parental RAM begins with the appearance of actively dividing cells in the parental QCL. These cells develop into the intervening initial cell files, which then separate the parental RAM into two daughters (Fig. 1q).

SAM has quiescent tissue and parental SAM splits into two daughter SAMs

To clarify tissue-level organisation, as well as meristem dynamics during branching, we

observed cell division activity in SAMs (Figs 2, S4; Table 2) based on the expression patterns of *histone H4*, a marker for cells undergoing DNA replication (Brandstädter *et al.*, 1994; Kouchi *et al.*, 1995; Meshi *et al.*, 2000). We also compared expression patterns of *histone H4* at successive stages of shoot branching with those of a *KNOX I* gene, which denote cell populations with meristematic competency (Harrison *et al.*, 2005; Atta *et al.*, 2009).

The parental shoot apex branched anisotomously to form small and large daughter apices (Fig. S1a). *KNOX I* was expressed throughout SAMs at stage 0 (Figs 2a, S4b, d). However, *histone H4* expression was detected mainly in the periphery of these SAMs, leading to an expression blank area at the centre of the SAM (Figs 2f, S4a, c). Cell division frequency was significantly lower in this blank area than in the surrounding SAM tissues throughout branching (Table 2).

The number of cells in SAM increased during stages 0 to IB, consistent with shoot tip expansion toward formation of a new apex (Table 2). At stage IA, the expression area of *KNOX I* expanded laterally (Figs 2b, S4j, l). The blank area, without *histone H4* expression, also broadened laterally at this stage and spots of *histone H4* expression were present at approximately one-third from the peripheral margin of the blank area (Figs 2g, S4i, k). Despite the appearance of these separating cells, fewer cell divisions

occurred in the blank area than in other parts of the SAM (Table 2). At stage IB, *KNOX I* expression was still observed throughout the SAM (Figs 2c, S4n, p), whereas two blank areas were observed to be separated by a mass of *histone H4* expressing cells (Figs 2h, S4m, o).

When the lateral shoot bulged at stage II, *KNOX I* expression was detected in both main and lateral SAMs (Figs 2d, S4t, v). At this stage, blank areas were also present in both main and lateral SAMs (Figs 2i, S4s, u; Table 2). Once the lateral shoot was completely isolated from the main shoot, *KNOX I* was again expressed throughout the SAM (Fig. 2e) and *histone H4* expression was less frequent in the central region (Fig. 2j).

Seed plant SAMs contain an organising centre (OC) with less frequent cell divisions (Dinneny & Benfey, 2008; Heidstra & Sabatini, 2014; Heyman *et al.*, 2014), which is visualised as a tissue devoid of *histone H4* expression signals (Brandstädter *et al.*, 1994; Kouchi *et al.*, 1995). Our *histone H4* expression data show that *Lycopodium* SAM also contains OC-like tissue (OCL). During shoot branching, separating cells appeared in the OCL which proliferated to divide the OCL into two daughters. As in RAMs, the behaviour of the OCL suggests that parental SAM splits to form two daughter SAMs (Fig. 2k).

To our knowledge, these data represent the first time that the SAM in lycophytes has been observed to contain tissue that resembles the OC in seed plants. Although the function of the OCL remains to be determined, we propose that the OCL is regulated differently than the OC in seed plants, because it includes the outermost cell layers of the SAM, which is contrary to the OC (Dinneny & Benfey, 2008; Heidstra & Sabatini, 2014; Heyman *et al.*, 2014).

Discussion

Meristematic dynamics suggest roots and shoots share fundamental body plans in *L. clavatum*

SAM dynamics during shoot branching were well illustrated by cell-lineage analyses in the lycophyte *Selaginella kraussiana* (Selaginellaceae) (Harrison *et al.*, 2007), but these data are not available for RAMs of this species. In addition, meristematic dynamics have not been clearly traced in SAMs and RAMs of other lycophyte species, despite many anatomical observation attempts made using classical histological techniques (Imaichi & Kato, 1989; Jernstedt *et al.*, 1992; Yi & Kato, 2001; Otreba & Gola, 2011). As a result, meristem dynamics have not been compared between SAMs and RAMs in a single lycophyte species. The molecular markers for DNA replications used in this

study enabled the comparison of meristematic dynamics in SAMs and RAMs of *L. clavatum*.

RAMs and SAMs of *L. clavatum* contained QCL and OCL, respectively, both of which were characterised by a lower frequency of cell division than that of the surrounding tissues (Figs 1, 2; Tables 1, 2). Although the QCL was covered by a root cap, it included the outermost tip of the root body (Fujinami *et al.*, 2017) (Fig. 1e, f), which was similar to the OCL (Fig. 2f). During dichotomous branching, a parental meristem divided to form two daughter meristems both in SAMs and RAMs of *L. clavatum*. Notably, RAM and SAM divisions began with the appearance of actively dividing cells within QCL (Fig. 1i, j) and OCL (Fig. 2g), respectively.

These data suggest that meristem organisation is strikingly similar between RAMs and SAMs and that they share common developmental mechanisms for dichotomous branching. Similarity in plasmodesmatal density also suggested that basic cellular characteristics are shared between RAMs and SAMs in *L. clavatum* (Imaichi & Hiratsuka, 2007; Imaichi *et al.*, 2018). It has been proposed that lycophyte roots may have evolved from the rooting axes of Early Devonian Drepanophycales or zosterophylls (Fig. 3) if they acquired a root cap (Kidston & Lang, 1921; Gensel & Berry, 2001; Gensel *et al.*, 2001; Hetherington & Dolan, 2018, 2019; but see also

below). This hypothesis suggests that roots are homologous to shoots in some extant lycophytes since the rooting axes are modified shoots, derived by a dichotomy of the shoot apex (Gensel & Berry, 2001; Gensel *et al.*, 2001). In addition, scale-like leaves were born on their basal part in *Asteroxylon mackiei* (Kidston & Lang, 1921). The developmental similarities between RAMs and SAMs of *L. clavatum* are consistent with a shoot origin for lycophyte roots. However, the rooting axes exogenously branched from parent stems (Gensel & Berry, 2001; Gensel *et al.*, 2001); therefore, the evolutionary process of endogeny should be explored in future studies to fill the gap between *Lycopodium* roots and rooting axes.

Roots and root-bearing organs may have evolved from Drepanophycales rooting axes

Among the three families comprising extant lycophytes (Kenrick & Crane, 1997; Wikström & Kenrick, 2001), Selaginellaceae and Isoetaceae have unique root-producing organs called rhizophores and rhizomorphs, respectively. These organs differ from shoots in their leafless nature, and differ from roots in that they are formed exogenously and lack a cap-like structure covering the apical meristem (Imaichi & Kato, 1989; Jernstedt *et al.*, 1992; Kenrick & Crane, 1997; Yi & Kato, 2001). Recent

transcriptome data indicated that *Selaginella* rhizophores exhibited an expression profile that differed from those of both roots and shoots (Mello *et al.*, 2019), suggesting that rhizophores have their own developmental process(es). In contrast, Lycopodiaceae does not have such root-producing organs and roots are typically produced endogenously from stems.

The rooting axes of Drepanophycales are similar to those root-producing organs in that they lack leaves and a cap-like structure, and are also produced exogenously (Gensel & Berry, 2001; Matsunaga & Tomescu, 2016, 2017; Hetherington & Dolan, 2018). Rooting axes may have produced roots laterally in the Early Devonian drepanophycalean lycophyte *Sengelia radicans* (Fig. 3; Matsunaga & Tomescu, 2016, 2017). These findings suggest that the rooting axes were the sources of different organs, potentially becoming roots in the *Lycopodium* lineage and root-producing organs in the *Sengelia* lineage (Fig. 3). Extant Selaginellaceae and Isoetaceae may therefore be descendants of the latter lineage.

Acknowledgements

This study was funded by Japan Society for the Promotion of Science (JSPS) KAKENHI grants (nos. 25870088 and 18K06380 to RF and no. 18H02495 to TY and

RF).

Authors' Contributions

RF, RI, and TY were involved in designing and conducting the entire study. TY constructed the conceptual framework for discussions of root evolution. AN performed anatomical observations. All authors read and approved the final version of the manuscript.

References

Atta R, Laurens L, Boucheron-Dubuisson E, Guivarc'h A, Carnero E, Giraudat-Pautot V, Rech P, Chriqui D. 2009. Pluripotency of *Arabidopsis* xylem pericycle underlies shoot regeneration from root and hypocotyl explants grown *in vitro*. *Plant Journal* **57**: 626–644.

Barlow PW. 1995. Structure and function at the root apex—phylogenetic and ontogenetic perspectives on apical cells and quiescent centres. In: Baluska F, Ciamporova M, Gasparíková O, Barlow PW, eds. *Structure and Function of Roots*. Dordrecht, Netherlands: Kluwer, 3–18.

van den Berg C, Willemsen V, Hendriks G, Weisbeek W, Scheres B. 1997. Short-range control of cell differentiation in the Arabidopsis root meristem. *Nature* **390**: 287–289.

Brandstädter J, Rossbach C, Theres K. 1994. The pattern of histone H4 expression in

the tomato shoot apex changes during development. *Planta* 192: 69–74.

Clowes FAL. 1961. *Apical meristems*. Oxford, UK: Blackwell.

Dinneny JR, Benfey PN. 2008. Plant stem cell niches: standing the test of time. *Cell* **132**: 553–557.

Dolan L, Janmaat K, Willemsen V, Linstead P, Poethig S, Roberts K, Scheres B. 1993. Cellular organisations of the *Arabidopsis thaliana* root. *Development* **119**: 71–84.

Doyle JA. 1998. Phylogeny of vascular plants. *Annual Review of Ecology, Evolution, and Systematics* **29**: 567–599.

Esau K. 1965. *Plant anatomy, 2nd edn*. New York, NY, USA, London, UK & Sydney, Australia: Wiley & Sons.

Friedman WE, Moore RC, Purugganan MD. 2004. The evolution of plant development. *American Journal of Botany* **91**: 1726–1741.

Fujinami R, Yamada T, Imaichi R. 2020. Root apical meristem diversity and the origin of roots: insights from extant lycophytes. *Journal of Plant Research* **133**: 291–296.

Fujinami R, Yamada T, Nakajima A, Takagi S, Idogawa A, Kawakami E, Tsutsumi M, Imaichi R. 2017. Root apical meristem diversity in extant lycophytes and implications for root origins. *New Phytologist* **215**: 1210–1220.

Gensel PG, Berry CM. 2001. Early lycophyte evolution. *American Fern Journal* **91**: 74–98.

Gensel PG, Kotyk ME, Basinger JF. 2001. Morphology of above- and below- ground structures in Early Devonian (Pragian-Emsian) plants. In: Gensel PG, Edwards D, eds. *Plants invade the land*. New York, NY, USA: Columbia University

Press, 83–102.

Gifford EM, Foster AS. 1989. *Morphology and evolution of vascular plants*, *3rd edn.* New York, NY, USA: W. Freeman.

Hao S, Xue J, Guo D, Wang D. 2010. Earliest rooting system and root: shoot ratio from a new *Zosterophyllum* plant. *New Phytologist* **185**: 217–225.

Harrison CJ, Corley SB, Moylan EC, Alexander DL, Scotland RW, Langdale JA. 2005. Independent recruitment of a conserved developmental mechanism during leaf evolution. *Nature* **434**: 509–514.

Harrison CJ, Rezvani M, Langdale JA. 2007. Growth from two transient apical initials in the meristem of *Selaginella kraussiana*. *Development* **134**: 881–889.

Heidstra R, Sabatini S. 2014. Plant and animal stem cells: similar yet different. *Nature Reviews Molecular Cell Biology* **15**: 301–312.

Hetherington AJ, Dolan L. 2017. The evolution of lycopsid rooting structures: conservatism and disparity. *New Phytologist* **215**: 538–544.

Hetherington AJ, Dolan L. 2018. Stepwise and independent origins of roots among land plants. *Nature* **561**: 235–238.

Hetherington AJ, Dolan L. 2019. Rhynie chert fossils demonstrate the independent origin and gradual evolution of lycophyte roots. *Current Opinion in Plant Biology* **47**: 119–126.

Heyman J, Kumpf RP, de Veylder L. 2014. A quiescent path to plant longevity. *Trends in Cell Biology* **24**: 443–448.

Hueber FM. 1992. Thoughts on the early lycopsids and zosterophylls. *Annals of the Missouri Botanical Garden* **79**: 474–499.

Imaichi R. 2008. Meristem organization and organ diversity. In: Ranker TA, Haufler

CH, eds. *Biology and Evolution of Ferns and Lycophytes*. Cambridge, UK: Cambridge University Press, 75–103.

Imaichi R, Hiratsuka R. 2007. Evolution of shoot apical meristem structures in vascular plants with respect to plasmodesmatal network. *American Journal of Botany* **94**: 1911–1921.

Imaichi R, Kato M. 1989. Developmental anatomy of the shoot apical cell, rhizophore and root of *Selaginella uncinata*. *Botanical Magazine Tokyo* **102**: 369–380.

Imaichi R, Moritoki N, Solvang HK. 2018. Evolution of root apical meristem structures in vascular plants: plasmodesmatal networks. *American Journal of Botany* **105**: 1453–1468.

Jernstedt JA, Cutter EG, Gifford EM, Lu P. 1992. Angle meristem origin and development in *Selaginella martensii*. *Annals of Botany* **69**: 351–363.

Kenrick P, Crane PR. 1997. *The origin and early diversification of land plants.* Washington, D.C., USA & London, UK: Smithsonian Institution Scholarly Press.

Kenrick P, Strullu-Derrien C. 2014. The origin and early evolution of roots. *Plant Physiology* **166**: 570–580.

Kerp H, Wellman CH, Krings M, Kearney P, Hass H. 2013. Reproductive organs and in situ spores of *Asteroxylon mackiei* Kidston & Lang, the most complex plant from the Lower Devonian Rhynie Chert. *International Journal of Plant Sciences* **174**: 293–308.

Kidston R, Lang WH. 1921. On Old Red Sandstone plants showing structure, from the Rhynie Chert Bed, Aberdeenshire. Part IV. Restorations of the vascular cryptogams, and discussion on their bearing on the general morphology of the

pteridophyta and the origin of the organization of land-plants. *Transactions of the Royal Society of Edinburgh* **52**: 831–854.

Kirschner GK, Stahl Y, Von Korff M, Simon R. 2017. Unique and conserved features of the barley root meristem. *Frontiers in Plant Science* **8**: 1240.

Kouchi H, Sekine M, Hata S. 1995. Distinct classes of mitotic cyclins are differentially expressed in the soybean shoot apex during the cell cycle. *Plant Cell* 7: 1143–1155.

Kumar S, Stecher G, Li M, Knyaz C, Tamura K. 2018. MEGA X: Molecular Evolutionary Genetics Analysis across computing platforms. *Molecular Biology and Evolution* **3**5: 1547–1549.

Le Hir G, Donnadieu Y, Goddéris Y, Meyer-Berthaud B, Ramstein G, Blakey RC. 2011. The climate change caused by the land plant invasion in the Devonian. *Earth and Planetary Science Letters* **310**: 203–212.

Matsunaga KKS, Tomescue AMF. 2016. Root evolution at the base of the lycophyte clade: insights from an early Devonian lycophyte. *Annals of Botany* **117**: 585–598.

Matsunaga KKS, Tomescu AMF. 2017. An organismal concept for *Sengelia radicans* gen. et sp. nov. – morphology and natural history of an Early Devonian lycophyte. *Annals of Botany* **119**: 1097–1113.

Mello A, Efroni I, Rahni R, Birnbaum KD. 2019. The *Selaginella* rhizophore has a unique transcriptional identity compared with root and shoot meristems. *New Phytologist* **222**: 882–894.

Meshi T, Taoka K, Iwabuchi M. 2000. Regulation of histone gene expression during cell cycle. *Plant Molecular Biology* **43**: 643–657.

Otręba P, Gola EM. 2011. Specific intercalary growth of rhizophores and roots in *Selaginella kraussiana* (Selaginellaceae) is related to unique dichotomous branching. *Flora* **206**: 227–232.

Poschmann M, Gossmann R, Matsunaga KKS, Tomescu AMF. 2020. Characterizing the branching architecture of drepanophycalean lycophytes (Lycopsida): an exceptional specimen from the Early Devonian Hunsrück Slate, southwest Germany, and its paleobiological implications. *PalZ* **94**: 1–16.

Raven JA, Edwards D. 2001. Roots: evolutionary origins and biogeochemical significance. *Journal of Experimental Botany* **52**: 381–401.

Rothwell GW, Erwin DM. 1985. The rhizomorph apex of *Paurodendron*: implications for homologies among the rooting organs of Lycopsida. *American Journal of Botany* **72**: 86–98.

Salic A, Mitchison TJ. 2008. A chemical method for fast and sensitive detection of DNA synthesis in vivo. *Proceedings of the National Academy of Sciences, USA* **105**: 2415–2420.

Talavera G, Castresana J. 2007. Improvement of phylogenies after removing divergent and ambiguously aligned blocks from protein sequence alignments. *Systematic Biology* **56**: 564–577.

Yamada T, Yokota S, Hirayama Y, Imaichi R, Kato M, Gasser CS. 2011. Ancestral expression patterns and evolutionary diversification of YABBY genes in angiosperms. *Plant Journal* **67**: 26–36.

Yi S, Kato M. 2001. Basal meristem and root development in *Isoetes asiatica* and *Isoetes japonica*. *International Journal of Plant Sciences* **162**: 1225–1235.

Yin X, Meicenheimer RD. 2017. Anisotomous dichotomy results from an unequal

bifurcation of the original shoot apical meristem in *Diphasiastrum digitatum* (Lycopodiaceae). *American Journal of Botany* **104**: 782–786.

Wikström N, Kenrick P. 2001. Evolution of Lycopodiaceae (Lycopsida): estimating divergence times from *rbcL* gene sequences by use of nonparametric rate smoothing. *Molecular Phylogenetic and Evolution* **19**: 177–186.

Supporting information

Fig. S1. Branching patterns in shoots and roots of *Lycopodium clavatum*.

Fig. S2. Images of *Lycopodium clavatum* root apical meristem used to measure size and count nuclei.

Fig. S3. Phylogenetic tree of KNOX genes based on the neighbour-joining method.

Fig. S4. *Histone H4* and *KNOX I* expression in *Lycopodium clavatum* shoot apical meristem (SAM).

Fig. S5. Negative controls used to analyse *in situ* hybridisation and cell division activity in *Lycopodium clavatum* root apical meristem (RAM).

Table S1. First branching types and distances between the first two third-order roots in *Lycopodium clavatum*.

Table S2. Measurement data for root tips shown in Fig. S2.

Table S3. Measurement data for shoot tips shown in Fig. S4.

Table S4. Primers used in this study.

Figure legennds

Fig. 1 (a–c) Young root systems of *Lycopodium clavatum* in which each second-order root forms a pair of third-order roots. (d) Distances between the first pair of third-order roots. (e–p) Cell division dynamics during root apical meristem (RAM) fission in *L. clavatum*. Red and white solid lines indicate boundaries between initial cell files around the quiescent centre-like tissue (QCL). Dashed lines indicate the boundary between the root body and the root cap. (e, g, i, k, m, o) 5-ethynyl-2′-deoxyuridine (EdU) signals (green florescence) in longitudinal median and four adjacent sections were superimposed onto phase-contrast image of the median one to cover all EdU-positive nuclei contained within the observed cells. (f, h, j, l, n, p) Merged images of 4',6-diamidino-2-phenylindole (DAPI) (blue florescence) and EdU signals observed on longitudinal median section. (e, f) Stage 0. (g–j) Stage I. (i, j) A group of actively

dividing cells appears in the QCL. (k, l) Stage II. Layered tissue is formed between the two incipient daughter QCLs. (m, n) Two RAMs are recognisable histologically and QCL is present in each daughter RAM. (o, p) RAM of the second-order root undergoing trichotomous-like branching. Two groups of EdU-positive cells appeared in the QCL (asterisks). (q) Schematic drawings summarising RAM division. Quiescent tissues (i.e., areas of infrequent cell division) are indicated by blue and meristematic regions include blue and pink coloured tissues. Red dots indicate EdU-positive cells separating the QCL. Scale bars: (a–c) 5 mm; (e–p) 50 μm.

Fig. 2 *KNOX I* (a–e) and *histone H4* (f–j) expression in *Lycopodium clavatum* at successive stages of shoot branching. (a, f) Stage 0. (b, g) Stage IA. Separating cells are indicated by red asterisks. (c, h) Stage IB. (d, i) Stage II. Bulge of the lateral (arrows). (e, j) Close-up of the lateral shoot apex after branching from the main axis. (k) Schematic drawings summarising shoot apical meristem division. Separating cells are indicated by red dots. Quiescent tissues (i.e., blank areas of *histone H4* expression) are indicated by blue and meristematic regions include blue and pink coloured tissues. All scale bars represent 50 μm.

Fig. 3 Possible evolutionary courses from subterranean shoot (rooting axis) of early lycophytes to root of *Lycopodium* and root-bearing organs of other extant lycophytes (indicated by arrows with a question mark). Ancestral condition of rooting axis is based on Gensel & Berry (2001).

Table 1 Cell data for root apical meristems (RAMs) and quiescent centre-like tissues (QCLs) of *Lycopodium clavatum*.

	Stage 0 (n=4)	Stage I			Stage II (n=5)	Stage II daughters (n=10)
		total (n=7)	-EdU (n=4)	+EdU (n=3)		
Width of root tips (μm)	510.3 ± 116.7	556.5 ± 78.8	588.7 ± 94.7	513.4 ± 17.0	617.4 ± 59.0	–
Length of root tips (μm)	142.7 ± 37.4	132.9 ± 15.0	139.7 ± 16.5	123.9 ± 7.3	144.4 ± 19.3	–
Width/length ratio of root tips	3.60 ± 0.20	4.18 ± 0.17[a]	4.20 ± 0.22[a]	4.15 ± 0.12	4.30 ± 0.29[a]	–
Nuclei in RAMs	465.8 ± 25.8	520.9 ± 48.0[b]	489.3 ± 16.6	563.0 ± 42.91[a]	724.6 ± 67.3[a, c]	–
Nuclear density in root tips (number/10^4 μm^2)	50.4 ± 18.9	57.0 ± 17.0	47.6 ± 9.3	69.0 ± 17.8[b]	63.7 ± 13.4	–
Cell division frequencies in root tips (excluding QCLs) (%)	15.8 ± 5.2	32.9 ± 13.0[b]	31.2 ± 14.4	35.5 ± 13.4	22.6 ± 9.2	–
Cell division frequencies in QCLs (%)	4.6 ± 0.8[*]	7.5 ± 3.1[**]	6.9 ± 4.1[*]	8.2 ± 1.5[b]	–	10.6 ± 4.2[**, a]
Width of QCLs (μm)	83.9 ± 31.3	76.3 ± 9.0	73.9 ± 10.5	79.4 ± 7.4	–	81.3 ± 11.6
Length of QCLs (μm)	82.4 ± 27.6	103.2 ± 17.4	102.9 ± 23.6	103.6 ± 8.3	–	75.6 ± 10.3[d]
Width/length ratio of QCLs	1.00 ± 0.11	1.35 ± 0.10[a]	1.38 ± 0.12[a]	1.31 ± 0.02[a]	–	1.09 ± 0.18[c]
Nuclei in QCLs	53.0 ± 18.3	63.1 ± 16.9	51.3 ± 6.8	79.0 ± 11.3[d]	–	41.7 ± 8.3[d]
Nuclear density in QCLs (number/10^4 μm^2)	28.5 ± 14.5	27.1 ± 5.5	24.4 ± 5.7	30.6 ± 2.8	–	22.0 ± 4.4

Measured values are shown in the form of 'mean ± SD'. Note that each root tip includes two incipient QCLs in stage II (–, not applicable). Among seven roots observed for stage I, a group of 5-ethynyl-2′-deoxyuridine (EdU)-positive cells were found in three roots (+EdU), but not in the remaining four (-EdU). Asterisks show that cell division

frequencies are significantly different (based on Student's t-test) between QCLs and non-QCL tissues within the same stage (**, $p < 0.01$; *, $p < 0.05$); a and b indicate significant differences from Stage 0 based on Welch's t-test (a, $p < 0.01$; b, $p < 0.05$); c and d indicate significant differences from the previous stage based on Welch's t-test (c, $p < 0.01$; d, $p < 0.05$).

Table 2 Cell data for shoot apical meristems (SAMs) and organising centre-like tissues (OCLs) of *Lycopodium clavatum*.

	Stage 0 (n=3)	Stage IA (n=3)	Stage IB (n=3)	Stage II (n=3)
Maximum width of shoot tips (μm)	285.9 ± 72.8	263.3 ± 36.3	316.7 ± 28.9	269.7 ± 31.0
Length of shoot tips (μm)	117.2 ± 31.4	77.7 ± 6.9	101.7 ± 9.9	113.2 ± 6.6
Width/length ratio of shoot tips	2.45 ± 0.16	3.38 ± 0.31	3.11± 0.03	2.38 ± 0.24
Cells in main SAMs[2]	177.7 ± 11.2	228.3 ± 25.4	282.7 ± 5.7[a]	193.0 ± 28.8[b]
Cells in main OCLs[1, 2]	31.7 ± 8.7	70.7 ± 19.9	45.0 ± 10.0	46.3 ± 18.8
Cell division frequencies in main SAMs (excluding OCLs) (%)	64.3 ± 12.2	52.5 ± 2.5	53.8 ± 8.9	42.2 ± 4.8
Cell division frequencies in main OCLs (%)	22.6 ± 4.2[*]	16.3 ± 5.4[**]	17.2 ± 7.4[**]	19.5 ± 3.1[*]
Cells in daughter SAMs[2]	–	–	–	76.0 ± 9.8
Cells in daughter OCLs[2]	–	–	25.0 ± 5.0	33.7 ± 4.0
Cell division frequencies in daughter SAMs (excluding OCLs) (%)	–	–	–	52.1 ± 5.9
Cell division frequencies in daughter OCLs (%)	–	–	18.2 ± 9.1[**]	25.4 ± 4.8[*]
Separating cells	–	11.3 ± 4.0	45.3 ± 19.1	–

Measured values are shown in the form of 'mean ± SD'. 1, OCLs correspond to blank areas with less frequent *histone H4* expression. 2, Parental SAM was branched between stages IB and II; OCLs were split between stages IA and IB. Asterisks show that cell division frequencies are significantly different (based on Student's t-test) between OCLs

and non-OCL tissues within the same stage (**, $p < 0.01$; *, $p < 0.05$); a and b indicate significant differences from Stage 0 based on Welch's t-test (a, $p < 0.01$; b, $p < 0.05$).

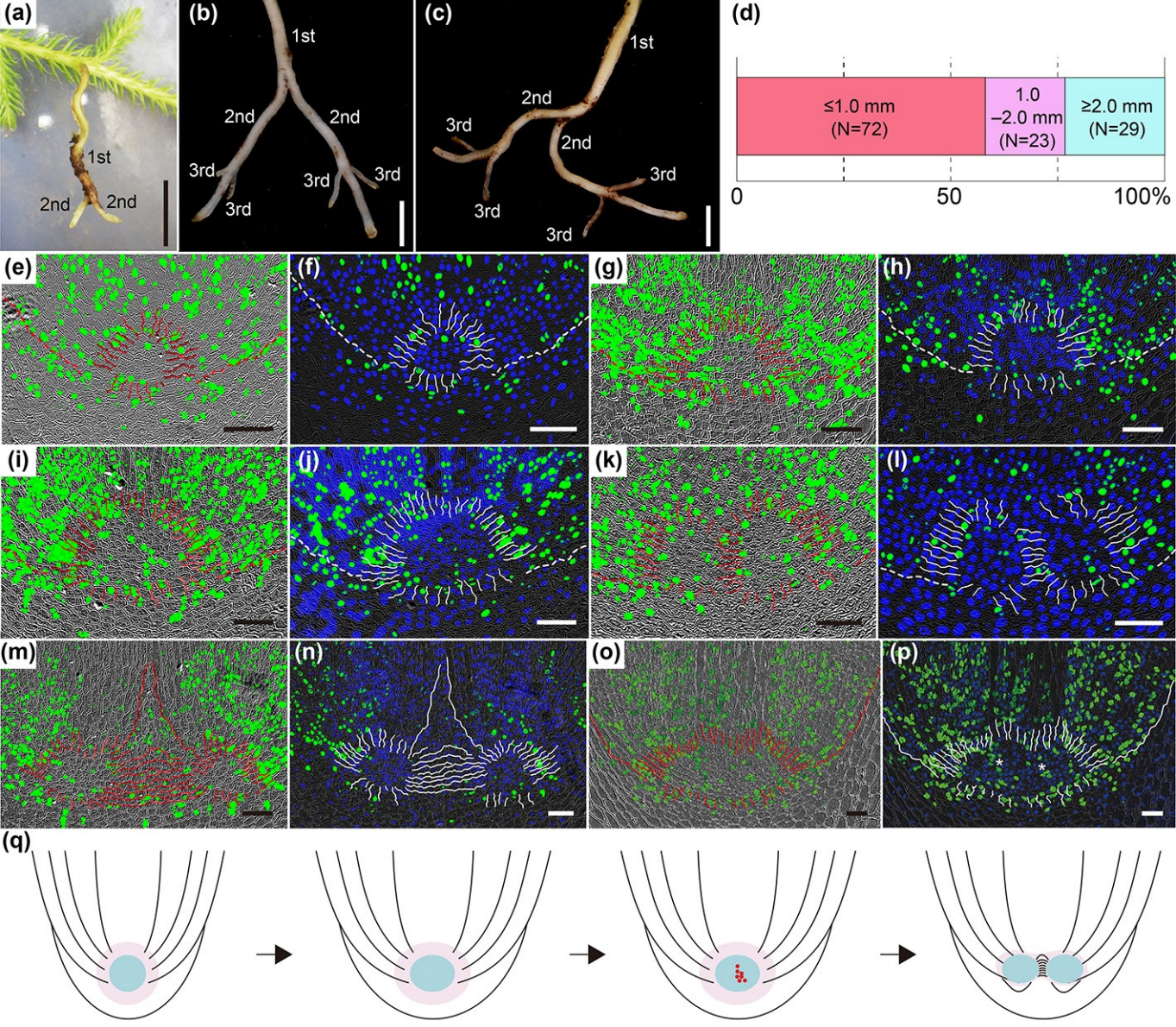
(a)
1st
2nd
2nd
(b)
1st
2nd
2nd
3rd
3rd
3rd
3rd
(c)
1st
2nd
3rd
2nd
3rd
3rd
3rd
(d)
≤1.0 mm
(N=72)
1.0
–2.0 mm
(N=23)
≥2.0 mm
(N=29)
0
50
100%
(e)
(f)
(g)
(h)
(i)
(j)
(k)
(l)
(m)
(n)
(o)
(p)
(q)

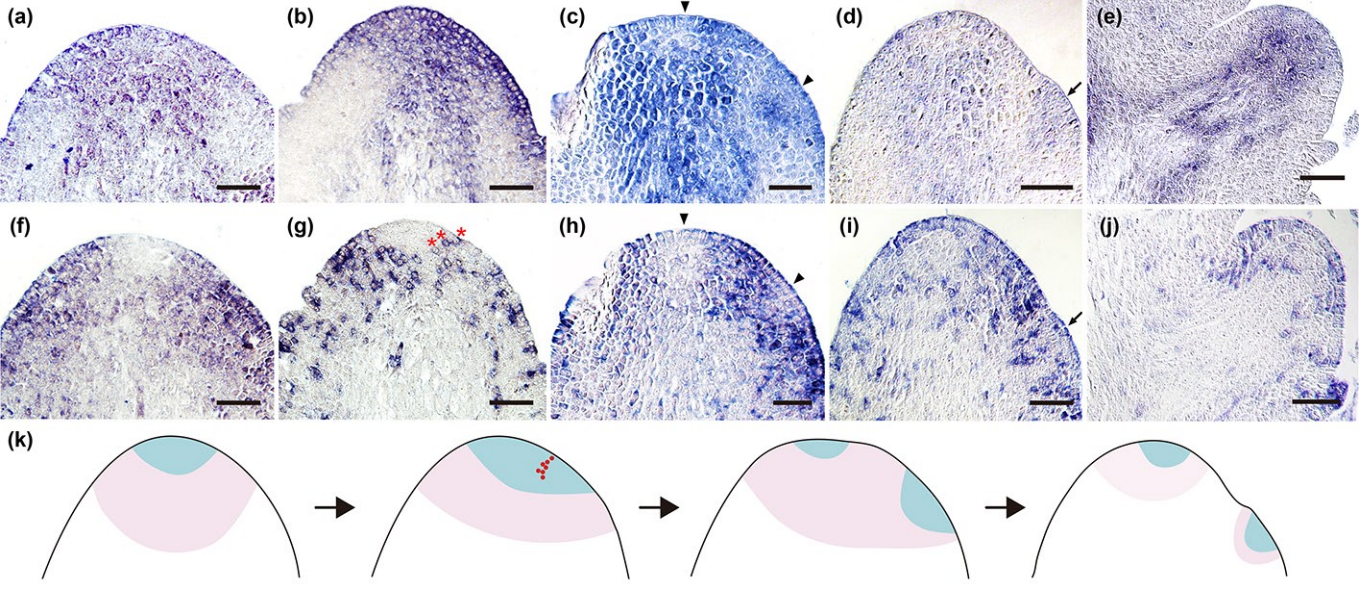
(a)
(b)
(c)
(d)
(e)
(f)
(g)
(h)
(i)
(j)
(k)

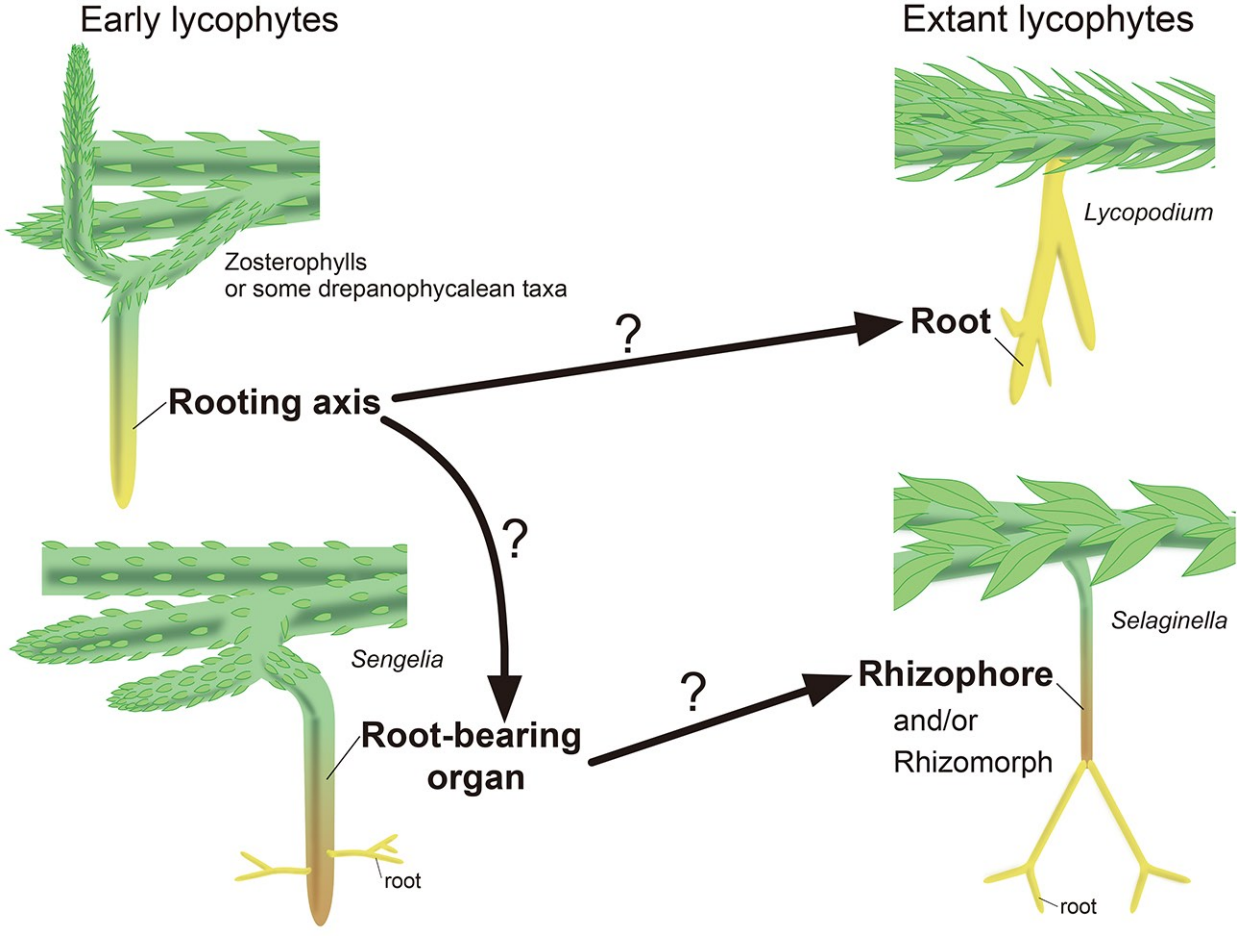
Early lycophytes
Extant lycophytes
Zosterophylls
or some drepanophycalean taxa
Lycopodium
?
Root
Rooting axis
?
Sengelia
Selaginella
?
Rhizophore
and/or
Rhizomorph
Root-bearing
organ
root
root